

Electron spin resonance study of copper(II) hydrogenmalonate dihydrate complex

S. MARCZYŃSKI¹, J. TYPEK^{1*}, N. GUSKOS^{1,2}, E. GRECH³, B. KOŁODZIEJ³

¹Institute of Physics, Szczecin University of Technology, al. Piastów 17, 70-310 Szczecin, Poland

²Solid State Physics, Department of Physics, University of Athens, Panepistimiopolis, 15 784 Zografos, Athens, Greece

³Department of Inorganic and Analytical Chemistry, Szczecin University of Technology, al. Piastów 17, 70-310 Szczecin, Poland

Copper(II) hydrogenmalonate dihydrate complex has been studied by using the electron spin resonance (ESR) method. Numerically deconvoluted ESR spectra of Cu(II) ions have been investigated at 4.2–295 K temperature range. The powder ESR spectrum has been described by three *g*-factors and additionally 1.5% of the existing spurious phases of a copper(II) complex has been revealed. The temperature dependence of the integrated ESR intensity has shown a Curie–Weiss type behaviour, consisting of two terms with different Curie–Weiss temperatures. The observed ferromagnetic interactions suggest the presence of two different paramagnetic species. It is proposed that the $[\text{Cu}(\text{H}_2\text{O})_4][\text{Cu}(\text{mal})_2(\text{H}_2\text{O})_2]$ copper(II) dimer complex is responsible for the low-temperature ($T < 50$ K) behaviour of the investigated sample.

Key words: *copper complex; ESR; malonate complex*

1. Introduction

Synthesis of ferro- and ferrimagnetic systems with a tunable T_c and three-dimensional (3D) ordering from molecular precursors including transition metal ions is one of the active branches of molecular inorganic chemistry [1–3]. The nature of interactions between transition metal ions (or transition metal ions and radicals) is rather complicated because it involves electrostatic (orbital) and magnetic (mainly dipolar) interactions. Therefore, the systems fulfilling necessary requirements to exhibit expected magnetic properties are not easy to design. There is a continued interest in the structural chemistry of copper(II) malonate, $\text{Cu}(\text{O}_2\text{CCH}_2\text{CO}_2)$ because of extensive use of malonate ions in the crystal engineering [4–6]. Malonate is a flexible and

*Corresponding author, e-mail: Janusz.Typek@ps.p1

versatile ligand. The structural complexity of malonate complexes is due to the ability of this dicarboxylate ligand, different from other dicarboxylic ligands, to adopt several chelating bidentate and/or different carboxylato-bridging coordination modes. The ability of the carboxylate bridge to mediate significant ferro- or antiferromagnetic coupling between paramagnetic centres is used to design materials with extended magnetic interactions [7–9]. Additionally, the group provides an efficient pathway coupling magnetic centres depending on structural aspects of metal environment [10–12].

Copper(II) malonate complexes with the formula $\text{Cu}(\text{C}_3\text{H}_2\text{O}_4) \times n\text{H}_2\text{O}$, where $n = 0, 1, 2, 2.5, 3, 4$ have been reported previously [13–17]. The number of water molecules influences the structural function of the malonate ions, which are bidentate in $n = 4$ complex and reveal tridentate-bridging function in $n = 3$ and $n = 2$ complexes. The type of structure changes from isolated complexes for $n = 4$ to a one-dimensional polymer for $n = 2$ complexes [5]. The reason for the variety of products from reaction between copper(II) salts and malonic acid is attributed to the conditions of the synthesis, pH value, stoichiometry and temperature. Also important is the a symmetry of the malonate dianion which cannot, for example, pack across the centre of inversion in solids.

The aim of this temperature ESR study of copper(II) hydrogenmalonate dihydrate ($\text{Cu}(\text{mal})_2(\text{H}_2\text{O})_2$, henceforth abbreviated as CuHM), is to reveal its magnetic properties. The ESR spectrum of powder samples of this compound will be analysed and fitted with an appropriate combination of single ESR lines. The obtained thermal dependence of the ESR parameters will be used to draw conclusion on the magnetic content of the studied sample.

2. Experimental

Crystals of CuHM were grown by a slow evaporation of aqueous solutions prepared by dissolving stoichiometric amounts of malonic acid and copper carbonate in water. The obtained deep-blue small single crystals were in the form of prisms. Powder samples were prepared by grinding a large number of small crystallites.

ESR measurements were carried out in a standard X band Bruker E 500 spectrometer. The spectrometer was equipped with TE_{102} cavity with 100 kHz field modulation. The investigated samples were in the form of powder and were placed in 4 mm diameter quartz tubes. ESR detected the power P absorbed by the sample from the transverse magnetic microwave field as a function of the static magnetic field H . The signal-to-noise ratio was improved by recording the derivative dP/dH using the lock-in technique with field modulation. An Oxford flow cryostat was used for temperature-dependent measurements in the 4–300 K temperature range.

3. Results and discussion

The CuHM compound, with the chemical formula $\text{Cu}(\text{C}_3\text{H}_2\text{O}_4) \times 2\text{H}_2\text{O}$, crystallizes in the monoclinic $P2_1/n$ space group [4]. Figure 1 presents a schematic representation

of the CuHM complex. In the structure of the title compound, the hydrogen malonate ions are almost planar. In the Cu complex, the metal coordination clearly shows the geometrical pattern typical of the Jahn–Teller effect [4].

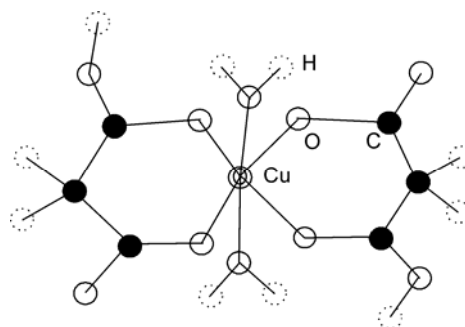


Fig. 1. Schematic representation of the formula of the CuHM complex

The ESR spectrum of a single crystal of CuHM at room temperature consists of an intense, single line without a hyperfine structure; its position strongly varies with the orientation of the sample in an external magnetic field. The lack of the hyperfine structure could indicate that the signal does not originate from isolated paramagnetic copper(II) ions. It is thus possible that the ions are strongly coupled by the exchange interaction (ferromagnetic or antiferromagnetic). Large exchange narrowing effects could suppress the hyperfine splitting. To examine the lineshape of that line, the derivative absorption signal was analysed and the result is shown in Fig. 2.

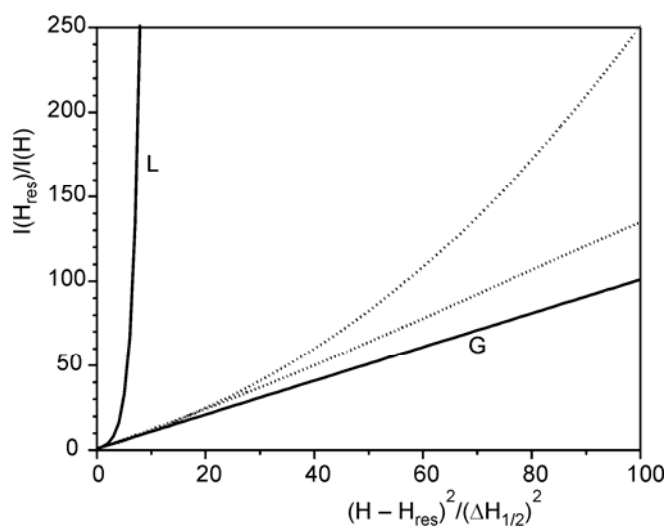


Fig. 2. ESR lineshape analysis of the CuHM single crystal at room temperature. The left- and right-hand side of the experimental CuHM line is represented by the dotted lines. Lorentzian (L) and Gaussian (G) type lines (solid lines) are presented for reference

The figure with an ordinate and an abscissa given as that in Fig. 2 is convenient, because the Lorentzian lineshape is reproduced as a straight line, as first introduced in [18]. In this figure, $I(H)$ is the height of the derivative line, $\Delta H_{1/2}$ is the halfwidth of the absorption curve, and H_{res} is the resonance field. For reference, the line which arises from Gaussian lineshape, which falls off much faster in the wings, is also given in Fig. 2. The recorded spectrum of CuHM is slightly asymmetric and its lineshape is close to Lorentzian.

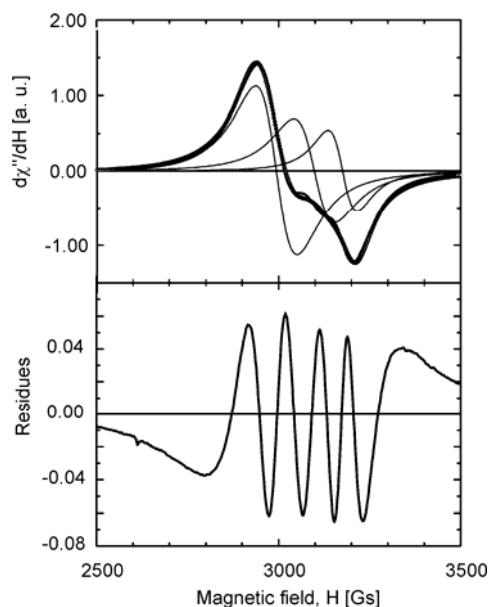


Fig. 3. ESR spectrum of the CuHM powder sample recorded at 50 K. Top panel – deconvolution of the experimental spectrum (circles) into three Lorentzian components (thin solid lines) and the sum of the three components (thick solid line). Lower panel – the difference between the experimental and fitted spectra

To simplify the procedure of the interpretation of the results, only the ESR measurements taken on the powder sample of CuHM will be further discussed. Figure 3 presents a typical recorded ESR spectrum of The CuHM complex at 50 K. The signal has been analysed in terms of being composed of three single Lorentzian lines (Fig. 3, top panel). The result of fitting of the observed ESR signal has been quite satisfactory. The effective g -factors of the components at room temperature are $g_1 = 2.254$, $g_2 = 2.184$, and $g_3 = 2.131$, and their peak-to-peak linewidths amount to 190 Gs, 195 Gs, and 140 Gs, respectively. The existence of these three different components reflects a low symmetry of the copper paramagnetic centre. Moreover, in the residue spectrum (Fig. 3, lower panel), calculated as the difference between the experimental spectrum and the fitted one, two additional signals could be discerned: one broad ($\Delta H = 200$ Gs), single line and other four-line spectrum superimposed on the former one, both centred at effective g -factor 2.20. The four-line spectrum resembles a typical Cu(II) ESR signal with the hyperfine structure arising from isolated paramagnetic centres. The integral intensity of those two spurious phases, and thus the number of paramagnetic impurities, constituted 1,5% of the total observed ESR signal.

The temperature evolution of the ESR spectra of CuHM powder sample is shown in Fig. 4. As the temperature is decreased from room temperature, the intensity of the ESR signal increases, but the overall shape of the spectrum remains roughly the same. To gain more insight into the nature of the paramagnetic centres producing the ESR signal, the temperature variation of the integrated intensity I has been studied. The integrated intensity is the area under the ESR absorption curve and can be calculated by double integration of the derivative ESR spectrum. This quantity is proportional to the susceptibility of the spins participating in the resonance.

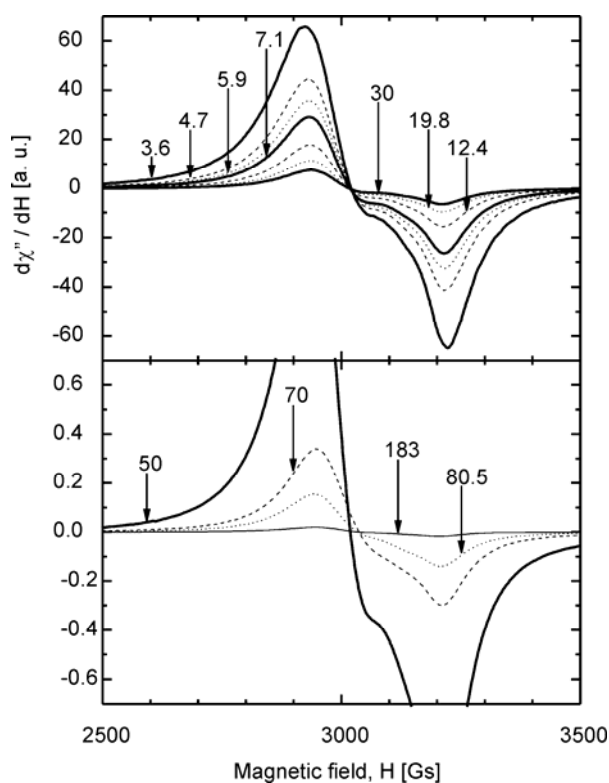


Fig. 4. Temperature evolution of the ESR spectra of the CuHM powder sample.

Top panel – low temperatures ($T < 50$ K),
lower panel – high temperatures ($T \geq 50$ K)

Figure 5 presents the temperature dependence of the integrated intensity (top panel), the temperature dependence of the reciprocal integral intensity (middle panel), and the product of temperature and the integrated intensity (bottom panel). The experimental data could not be satisfactorily fitted by the single Curie–Weiss law, but are fairly well represented by a sum of two Curie–Weiss terms:

$$I = C_1/(T - \Theta_1) + C_2/(T - \Theta_2) \quad (1)$$

The best fit of this function to experimental data (Fig. 5, lower panel) gave the following values of the Curie–Weiss temperatures: $\Theta_1 = 60(14)$ K, $\Theta_2 = 6.8(4.8)$ K. The positive sign of the Curie–Weiss temperature evidences for the ferromagnetic interactions between the copper paramagnetic centres. Another indication of the ferromagnetic interactions is the temperature behaviour of the product of temperature and integrated intensity. This quantity is proportional to the effective magnetic moment of the CuHM complex. On decreasing the temperature, the effective magnetic moment increases (Fig. 5, lower panel).

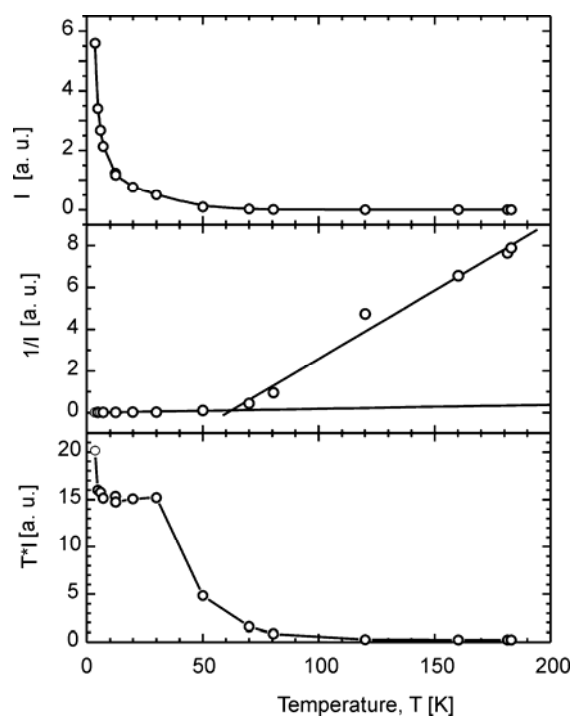


Fig. 5. Temperature dependence of the integrated ESR intensity of the CuHM complex (top panel), the reciprocal integrated intensity (middle panel), and the product of temperature and the integrated intensity (lower panel)

The experimental ESR spectrum of the CuHM complex taken at each temperature was decomposed into three Lorentzian components, and the ESR parameters of each component (the resonance field H_{res} and the peak-to-peak linewidth ΔH_{pp}) have been determined by the least-square fitting. The temperature variation of these parameters is presented in Fig. 6. A closer inspection of Fig. 6 allows to divide the temperature behaviour of magnetic properties of the CuHM complex into two ranges: a high temperature range ($T > 50$ K) and the low-temperature range ($T < 50$ K). In the high temperature range, the changes of resonance fields and linewidths of all three components are very small, if any, and in the low temperature range these parameters are subject

to significant variations. In general, the resonance fields of the components decrease as the temperature is decreased but their linewidths show a more complicated behaviour. The linewidth of the high-field component displays a rapid increase as the temperature is decreased (from 140 Gs at 50 K to 200 Gs at 10 K). It is interesting to note that the behaviour of linewidths of the middle- and low-field components is the same in the high-temperature range, while in the low-temperature range the lines behave oppositely. Shifting of the resonance fields to lower magnetic fields with decreasing temperature indicates on build-up of an internal magnetic field.

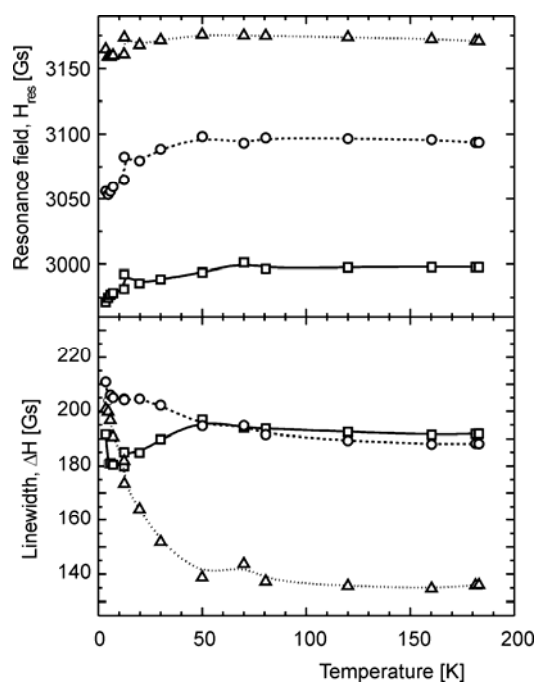


Fig. 6. Temperature dependence of the ESR parameters (resonance field H_{res} – upper panel, peak-to-peak linewidth ΔH – lower panel) of the three components constituting the resonance signal of the CuHM complex

The ESR linewidth in magnetic insulators is usually decomposed into noncritical and critical parts:

$$\Delta H = \Delta H(\infty) + \Delta H_{\text{crit}}(T) \quad (2)$$

The first term describes the spin–spin interactions in the high-temperature paramagnetic regime, where spins are uncorrelated. In concentrated paramagnetic systems, a constant contribution to the ESR linewidth is determined mainly by the isotropic exchange narrowing effect, magnetic and structural inhomogeneities, and anisotropic spin–spin interactions like, e.g., dipole–dipole interactions and anisotropic exchange [19].

The second term defines an additional contribution to ΔH appearing at low temperatures, when the long-range magnetic order is approached. It is caused by fluctuations of the staggered magnetization in the short-range ordered state. These enhance the spin–spin relaxation rate $1/T_2$ and, consequently, additionally broaden the ESR line [20].

All the above presented results of the ESR study indicate the existence of two types of bulk paramagnetic centres in the investigated sample. There is a ferromagnetic interaction operating in both centres, but with different strengths, which is reflected in different values of the Curie–Weiss temperatures. Although the presence of ferromagnetic interaction has been established, no long-range ferromagnetic order has been observed in the investigated temperature range $T > 4$ K. The behaviour of the high-field component in the low-temperature range points to approaching the long-range ferromagnetic order at $T < 4$ K. A comparison of the published magnetic properties of malonato-bridges copper complexes with recorded ESR behaviour (Fig. 6) suggests that a copper(II) dimer complex may be present in our sample. The coexistence of the monomer and dimer copper(II) complexes would also explain the observed temperature change of the integrated ESR intensity. The low-temperature behaviour of the investigated sample would thus be determined by the copper dimer phase.

The literature data shows that 95% of copper(II) dimers exhibit an antiferromagnetic coupling, but in malonato-bridged metallic complexes, the ferromagnetic coupling is more frequent [8]. The simplest compound with dinuclear copper(II) of this type is $[\text{Cu}(\text{H}_2\text{O})_4][\text{Cu}(\text{mal})_2(\text{H}_2\text{O})_2]$. The neutral dinuclear entity consists of a diaquabis(malonato)-cuprate(II) anion and a tetraaquacopper(II) cation connected through a carboxylato group. The environment of the chelated copper(II) ion is octahedral, whereas the coordination of the other is square pyramidal [1]. In square, pyramidal and octahedral environments, the magnetic orbital at each copper(II) atom is defined by short equatorial (or basal) bonds, and it is of the $d_{x^2-y^2}$ type with possible admixture of the d_{z^2} orbital in the axial position. In $[\text{Cu}(\text{H}_2\text{O})_4][\text{Cu}(\text{mal})_2(\text{H}_2\text{O})_2]$ dimer, the carboxylate couples a $d_{x^2-y^2}$ magnetic orbital of Cu(I) with a d_{z^2} nonmagnetic orbital of Cu(II), the latter being orthogonal to the former. This kind of coupling (basal-apical or equatorial-axial) is found in many compounds and is always ferromagnetic. The intradimer coupling constant for the $[\text{Cu}(\text{H}_2\text{O})_4][\text{Cu}(\text{mal})_2(\text{H}_2\text{O})_2]$ dimer is $J = 1.8 \text{ cm}^{-1}$ and the thermal dependence of its magnetic moment shows a significant increase below 50 K [1]. The presence of copper dimers in the sample is very probable the more so as this phase crystallizes in the same chemical and physical conditions as the monomer phase.

4. Conclusions

In conclusion, it has been shown that the investigated sample is magnetically inhomogeneous and consists mostly of a mixture of the $\text{Cu}(\text{mal})_2(\text{H}_2\text{O})_2$ monomer and

[Cu(H₂O)₄][Cu(mal)₂(H₂O)₂] dimer copper(II) complexes. Moreover, there is about 1.5% of other spurious phases. Both dominating constituents showed strong ferromagnetic interactions, but no long-range order above 4 K.

References

- [1] PASAN J., DELGADO F.S., RODRIGUEZ-MARTIN Y., HERNANDEZ-MOLINA M., RUIZ-PEREZ C., SANCHIZ J., LLORET F., JULVE M., *Polyhedron*, 22 (2003), 2143.
- [2] RODRIGUEZ-MARTIN Y., RUIZ-PEREZ C., SANCHIZ J., LLORET F., JULVE M., *Inorg. Chim. Acta*, 318 (2001), 159.
- [3] RODRIGUEZ-MARTIN Y., HERNANDEZ-MOLINA M., DELGADO F.S., PASAN J., RUIZ-PEREZ C., SANCHIZ J., LLORET F., JULVE M., *Cryst. Eng. Comm.*, 4 (2002), 522.
- [4] LENSTRA A.T.H., KATAEVA O.N., *Acta Cryst. B*, 57 (2001), 497
- [5] FILIPPOVA I.G., *Moldavian J. Phys. Sci.*, 1 (2002), 87
- [6] NAUMOV P., RISTOVA M., SOPTRAJANOV B., DREW M.G.B., NG S.W., *Croatica Chem. Acta*, 75 (2002), 701.
- [7] TOWLE D.K., HOFFMANN S.K., HATFIELD W.E., SING P., CHAUDHURI P., *Inorg. Chem*, 27 (1988), 394.
- [8] RUIZ-PEREZ C., RODRIGUEZ-MARTIN Y., HERNANDEZ-MOLINA M., DELGADO F.S., PASAN J., SANCHIZ J., LLORET F., JULVE M., *Polyhedron*, 22 (2003), 2111.
- [9] CHAWLA S.K., ARORA M., NATTINEN K., RISSANEN K., YAKHMI J.V., *Polyhedron*, 23 (2004), 3007.
- [10] OLDHAM C., [in:] *Comprehensive Coordination Chemistry*, G. Wilkinson, R.D. Gillard, J.A. McCleverty (Eds.), Vol. 2, Pergamon Press, Oxford, 1987, p. 435.
- [11] LEVSTEIN P.R., CALVO R., *Inorg. Chem.*, 29 (1990), 1581.
- [12] RUIZ E., *Inorg. Chem.*, 212 (1993), 115.
- [13] PLOQUIN J., *Bull. Soc. Chim. France*, 18 (1951), 757.
- [14] DUBICKI L., HARRIS C.M., KOKOT E., MARTIN R.L., *Inorg. Chem.*, 5 (1966), 93.
- [15] SIERON L., *Acta Cryst.*, 60 (2004), 297.
- [16] ASAI O., KISHITA M., KUBO M., *J. Phys. Chem.*, 63 (1959), 96.
- [17] RAJAN R., *J. Chem. Phys.*, 37 (1962), 460.
- [18] DIETZ R.E., MERRITT F.R., DINGLE R., HONE D., SILBERNAGEL B.G., RICHARDS P.M., *Phys. Rev. Lett.*, 26 (1971), 1186.
- [19] ABRAGAM A., BLEANEY B., *Electron Paramagnetic Resonance of Transition Ions*, Oxford University Press, Oxford, 1970.
- [20] HUBER D.L., *Phys. Rev. B*, 6 (1972), 3180.

Received 9 September 2005

Revised 23 November 2005